Low-Complexity Near-Optimum Multiple-Symbol Differential Detection of DAPSK Based on Iterative Amplitude/Phase Processing

Li Wang, *Member, IEEE* and Lajos Hanzo, *Fellow, IEEE*

Abstract

Differentially encoded and non-coherently detected transceivers exhibit a low complexity, since they dispense with complex channel estimation. In pursuit of high bandwidth efficiency, differential amplitude and phase shift keying (DAPSK) was devised using constellations of multiple concentric rings. In order to increase resilience against the typical high-Doppler-induced performance degradation of DAPSK and/or enhance the maximum achievable error-free transmission rate for DAPSK modulated systems, multiple-symbol differential detection (MSDD) may be invoked. However, the complexity of the maximum-a-posteriori (MAP) MSDD increases exponentially with the detection window size and hence may become excessive upon increasing the window size, especially in the context of iterative detection aided channel coded system. In order to circumvent this excessive complexity, we conceive a decomposed two-stage iterative amplitude and phase (A/P) detection framework, where the challenge of having a non-constant-modulus constellation is tackled with the aid of a specifically designed information exchange between the independent A/P detection stages, thus allowing the incorporation of reduced-complexity sphere detection (SD). Consequently, a near-MAP-MSDD performance can be achieved at a significantly reduced complexity, which may be five orders of magnitude lower than that of the traditional MAP-MSDD in the 16-DAPSK scenario considered.

I. Introduction

FUTURE wireless communications will have to support a high grade of mobility. The major candidates for the next generation of broadband wireless access systems, such as 3GPP-LTE and IEEE 802.16m, are expected to deliver a data rate of at least 100 Mbps for high-velocity mobile users (up to 350 km/h) [1, 2]. Differential phase shift keying (DPSK) relying on low-complexity non-coherent detection constitutes an attractive solution for high-mobility wireless communications, especially in scenarios, such as for example, cooperative communications, since it is robust against the phase ambiguities induced by rapid fading, while dispensing with channel estimation for mobile-to-mobile links. Thus, the employment of pilot symbols may be avoided in non-coherent transmissions.

The authors are with the school of ECS, University of Southampton, Southampton, SO17 1BJ, UK (e-mail: {lw5,lh}@ecs.soton.ac.uk).

The finacial support of the RC UK under the auspices of the UK-India Advanced Technology Centre of Wireless Communications and of the China-UK Science Bridge in 4G wireless communications, as well as that of the EU's Concerto project is also gratefully acknowledged.

For the sake of further improving the achievable spectral efficiency, differential amplitude and phase shift keying (DAPSK) [3, 4] expanded the single-ring constellation of the traditional DPSK to multiple rings. Essentially, the information bits are mapped to both the amplitude and phase differences between successively transmitted symbols.

In order to enhance the maximum achievable error-free transmission rate for a given DAPSK modulation as well as to eliminate the typical emergence of an error-floor at high Doppler-frequencies, the multiple-symbol differential detector (MSDD) has been applied to uncoded DAPSK-modulated systems in [5], which relies on the joint detection of multiple consecutively received symbols. However, when employed in an iterative detection aided channel coded DAPSK-aided system, the maximum-a-posteriori (MAP) soft-decision MSDD [6, 7] employing even a moderate observation window size N may still exhibit an excessive complexity, since it has to generate soft information based on the brute-force search for every transmitted bit. As a potential complexity reduction technique, the well-known tree-search-based sphere detection (SD) mechansim has been proposed for MSDD of a conventional DPSK modulated system [8], leading to the multiple-symbol differential sphere detection (MSDSD). Unfortunately, the non-constant-modulus constellation DAPSK precludes the direct application of the MSDSD scheme of [8]. Thus, until now the conception of an efficient MSDD for DAPSK-aided systems remained an open problem.

Against this background, firstly, we close this open problem by proposing an iterative A/P detection framework for MSDD-aided DAPSK systems; Secondly, the iterative information exchange between the above-mentioned A/P detection stages is specifically tailored for mitigating any potential performance penalty imposed by the separate A/P detection; Thirdly, we incorporate the SD mechanism in this new MSDD for the sake of further complexity reduction. Our simulation results demonstrate a near-MAP-MSDD performance can be achieved at a significantly reduced complexity, which may be five orders of magnitude lower than that imposed by the traditional MAP-MSDD in the 16-DAPSK scenario considered.

Notations: We use boldface variables to denote matrices as well as vectors and $\mathcal{E}\{\cdot\}$ for expectation. Furthermore, $v[m]$ is the mth element of the vector $\mathbf{v}$, while $\det(\mathbf{S})$ and $\mathbf{S}^{-1}$ are the determinant and inverse of a square matrix $\mathbf{S}$, respectively. For any general matrix $\mathbf{M}$, $\mathbf{M}^{\mathrm{H}}$ represents the conjugate transpose.

II. System Architecture & Channel Model

The simplified overall system model of bit-interleaved coded differential modulation is depicted in Fig. 1. At the transmitter of Fig. 1, a block of L information bits u is first encoded by the channel encoder in order to generate

the coded bits c, which are then interleaved by the interleaver π. The resultant permuted bits b are then fed through the DAPSK modulator. The 2^p-DAPSK, also known as the Star Quadrature Amplitude Modulation (Star-QAM) scheme [3], employs multiple concentric rings by combining the 2^q-DASK and $2^{(p-q)}$-DPSK modulation schemes. Specifically, as illustrated in Fig. 1, the first q bits, $\mathbf{b}_\gamma^n = [b_{\gamma,1}^n, \cdots, b_{\gamma,q}^n]$, of the nth p-bit encoded APSK symbol $d[n] = \gamma[n]v[n]$ are mapped to one of the legitimate radii $\mathcal{R} = \{\alpha^{i_\mathrm{A}} | \ i_\mathrm{A} = 0, \cdots, 2^q - 1\}$ in order to generate the component ASK symbol $\gamma[n]$, for example, according to the mapping schemes of Table I. Meanwhile, the remaining $(p-q)$ bits, $\mathbf{b}_\theta^n = [b_{\theta,1}^n, \cdots, b_{\theta,p-q}^n]$, are mapped to the component PSK symbol $v[n] = \mathrm{e}^{j\theta[n]} \in \mathcal{V} = \{\mathrm{e}^{j2\pi i_\mathrm{P}/2^{(p-q)}} | i_\mathrm{P} = 0, \cdots, 2^{(p-q)} - 1\}$. Based on the above ASK and PSK modulation, differential encoding of the resultant APSK symbol $d[n]$ may be performed, in order to generate the DAPSK symbol $x[n] = a[n]s[n]$ as:

$$x[n] = d[n] \odot x[n-1] = \gamma[n]v[n] \odot a[n-1]s[n-1], \tag{1}$$

$$= \alpha^{(i_\mathrm{A}\{\gamma[n]\} + i_\mathrm{A}\{a[n-1]\}) \bmod 2^q} \cdot \exp[j2\pi(i_\mathrm{P}\{v[n]\} + i_\mathrm{P}\{s[n-1]\})/2^{(p-q)}], \tag{2}$$

where $i_\mathrm{A}\{\cdot\}$ and $i_\mathrm{P}\{\cdot\}$ are the indices of the radius- and phase-arguments, respectively. We note that with the aid of the modulo-2^q operation, the transmitted component DASK symbol $a[n]$ is restricted to be taken from the same signal set as the ASK symbol $\gamma[n]$, i.e., $a[n] \in \mathcal{A} = \mathcal{R}$, as usual for DPSK, where we have $s[n] \in \mathcal{S} = \mathcal{V}$ due to the inherent periodicity of the phase. As an example, the signal constellation set $\mathcal{X}$ of 16-DAPSK ($p = 1, \ q = 4$) is depicted in Fig. 2, which is constituted of two concentric rings of 8-PSK symbols.

For the sake of simplicity, we consider the narrow-band time-selective Rayleigh fading channel, where the fading coefficients have an autocorrelation function of $\varphi[\kappa] \triangleq \mathcal{E}\{h[n+\kappa]h^*[n]\} = J_0(2\pi f_d \kappa)$, according to the widely-used Clarke model, with $J_0(\cdot)$ and f_d representing the zero-order Bessel function of first kind and the normalized Doppler frequency, respectively. Thus, the *single-symbol*-based transmission model may be expressed as $y[n] = h[n]x[n] + w[n]$, where $h[n]$ and $w[n]$ denote the fading coefficient obeying a complex Gaussian distribution of $\mathcal{CN}(0, \sigma_h^2)$ and the AWGN noise having a distribution of $\mathcal{CN}(0, 2\sigma_w^2)$, respectively. Then, the faded and noise-contaminated received symbol $y[n]$ is processed by the turbo receiver of Fig. 1 constructed by serially concatenating the differential detector as well as the channel decoder, and then exchanging *extrinsic* information between them. As shown in Fig. 1, $L_A(\cdot)$ represents the *a priori* information expressed in terms of the log-likelihood ratios (LLRs) [9], while $L_E(\cdot)$ denotes the corresponding *extrinsic* information.

III. Iterative Amplitude/Phase Multiple-Symbol Differential Detection

Conventional differential detection (CDD) techniques [6, 10–12] proposed for DAPSK rely on the direct calculation of the amplitude and phase differences, namely on $\lambda[n] = |y[n]|/|y[n-1]|$ and $\triangle\phi[n] = \angle y[n] - \angle y[n-1]$, respectively, between two consecutively received symbols. However, in pursuit of an improved maximum achievable error-free transmission rate and/or an increased resilience against the formation of a high-Doppler-induced error-floor, one has to exploit the correlation between the amplitude and phase distortions experienced by the consecutively transmitted symbols with the aid of multiple-symbol-based detection.

A. MAP-Based Multiple-Symbol Differential Detection

1) Principle of the MSDD: Briefly, the MSDD makes a decision about the k_Nth block of N consecutively transmitted DAPSK symbols $\mathbf{x}[k_N] = [x[k_N(N-1)], \cdots, x[(k_N+1)(N-1)]]^{\mathrm{T}}$ on the basis of N successively received symbols stored in $\mathbf{y}[k_N] = [y[k_N(N-1)], \cdots, y[(k_N+1)(N-1)]]^{\mathrm{T}}$. Since each element of $\mathbf{x}[k_N]$ is the product of the component DASK and DPSK symbols, we have $\mathbf{x}[k_N] = \mathbf{a}[k_N] \cdot \mathbf{s}[k_N]$ with the vectors $\mathbf{a}[k_N]$ and $\mathbf{s}[k_N]$ containing the corresponding N consecutively transmitted constituent DASK and DPSK symbols, respectively. Thus, a *multiple-symbol*-based transmission may be modeled as:

$$\mathbf{y}[k_N] = \mathbf{X}_{\mathrm{d}}[k_N]\mathbf{h}[k_N] + \mathbf{w}[k_N] = \mathbf{A}_{\mathrm{d}}[k_N]\mathbf{S}_{\mathrm{d}}[k_N]\mathbf{h}[k_N] + \mathbf{w}[k_N], \tag{3}$$

where $\mathbf{X}_{\mathrm{d}}[k_N] = \mathrm{diag}\{\mathbf{x}[\mathrm{k_N}]\}$, $\mathbf{A}_{\mathrm{d}}[k_N] = \mathrm{diag}\{\mathbf{a}[k_N]\}$ and $\mathbf{S}_{\mathrm{d}}[k_N] = \mathrm{diag}\{\mathbf{s}[k_N]\}$ are all diagonal matrices with their first upper-left element being the reference DAPSK symbol $x[k_N(N-1)] \triangleq x_{\mathrm{ref}} \in \mathcal{X}$, the reference component DASK symbol $a[k_N(N-1)] \triangleq a_{\mathrm{ref}} \in \mathcal{A}$ and the reference component DPSK symbol $s[k_N(N-1)] \triangleq s_{\mathrm{ref}} \in \mathcal{S}$, respectively. Additionally, $\mathbf{h}[k_N] = [h[k_N(N-1)], \cdots, h[(k_N+1)(N-1)]]^{\mathrm{T}}$ and $\mathbf{w}[k_N] = [w[k_N(N-1)], \cdots, w[(k_N+1)(N-1)]]^{\mathrm{T}}$ of (3) represent the fading coefficients' column vector obeying a complex-valued Gaussian distribution $\mathcal{CN}(0, \mathbf{\Sigma}_h)$ and the Gaussian noise column vector having a distribution of $\mathcal{CN}(0, 2\sigma_w^2\mathbf{I}_N)$, respectively. Note that $\mathbf{\Sigma}_h \triangleq \mathcal{E}\{\mathbf{h}\mathbf{h}^{\mathrm{H}}\}$ denotes the channel's covariance matrix.

Under the assumption that both the fading and noise are zero-mean complex Gaussian processes, the probability density function (PDF) of $\mathbf{y}[k_N]$ conditioned both on $\mathbf{\Gamma}[k_N] = [\gamma[k_N(N-1)], \cdots, \gamma[(k_N+1)(N-1)-1]]^{\mathrm{T}}$ and on $\mathbf{\Theta}[k_N] = [\theta[k_N(N-1)], \cdots, \theta[(k_N+1)(N-1)-1]]^{\mathrm{T}}$, i.e. $p(\mathbf{y}[k_N]|\mathbf{\Gamma}[k_N], \mathbf{\Theta}[k_N])$, can be expressed by averaging

$p(\mathbf{y}|\mathbf{X}_d)$ over all possible values of $x_{\rm ref}$ as follows (the block index k_N is omitted for notation simplicity):

$$p(\mathbf{y}|\mathbf{\Gamma},\mathbf{\Theta}) = \mathcal{E}_{x_{\rm ref}}\{p(\mathbf{y}|\mathbf{X}_{\rm d})\} = \mathcal{E}_{x_{\rm ref}}\left\{\frac{\exp\{-\mathbf{y}^{\rm H}[\Psi(\mathbf{X}_{\rm d})]^{-1}\mathbf{y}\}}{\pi^N \det[\Psi(\mathbf{X}_{\rm d})]}\right\}, \tag{4}$$

where the conditional autocorrelation matrix

$$\Psi(\mathbf{X}_{\rm d}) = \mathcal{E}\{\mathbf{y}\mathbf{y}^{\rm H}|\mathbf{X}_{\rm d}\} = \mathbf{X}_{\rm d}\mathbf{\Sigma}_h\mathbf{X}_{\rm d}^{\rm H} + 2\sigma_w^2\mathbf{I}_N \tag{5}$$

is dependent on the transmitted signal matrix $\mathbf{X}_{\rm d}$. The soft bit information expressed in terms of *a posteriori* LLRs may be calculated with the aid of the Bayes' theorem at the output of the MAP-MSDD as:

$$L_D(b_i^n|\mathbf{y}) = \ln\frac{\Pr(b_i^n=+1|\mathbf{y})}{\Pr(b_i^n=-1|\mathbf{y})} = \ln\frac{\sum_{\mathbf{b}\in\mathbb{B}_{n,i,+1}} p(\mathbf{y}|\mathbf{\Gamma},\mathbf{\Theta})\Pr(\mathbf{b})}{\sum_{\mathbf{b}\in\mathbb{B}_{n,i,-1}} p(\mathbf{y}|\mathbf{\Gamma},\mathbf{\Theta})\Pr(\mathbf{b})}, \tag{6}$$

where $\mathbb{B}_{n,i,\pm1}$ represents the set of $2^{(pN-1)}$ legitimate transmitted bit vectors $\mathbf{b}$ associated with the ith bit of the p-bit-coded symbol being $b_i^n = \pm 1$ ($i \in \{0,\cdots,p-1\}$). Note that in this treatise, the logical zero for a bit is represented by amplitude level $b=-1$, and a logical one by $b=+1$. In the sequel, the *extrinsic* LLR may be obtained by excluding the corresponding *a priori* LLR, $L_A(b_i^n) = \ln\frac{\Pr(b_i^n=+1)}{\Pr(b_i^n=-1)}$, from the *a posteriori* LLR, $L_D(b_i^n|\mathbf{y})$, which is exploited by the outer channel decoder after passing it through the deinterleaver as shown in Fig. 1.

2) Complexity of the MAP-MSDD: According to (4) and (6), the asymptotic complexity of the MAP-MSDD of a 2^p-DAPSK scheme using 2^q concentric rings is $\mathcal{O}(p\cdot 2^{(pN)})$. It is also noteworthy that for modulation schemes using constant-modulus constellation, such as DPSK, $p(\mathbf{y}|\mathbf{X}_d)$ is independent of $x_{\rm ref}$, hence the averaging in (4) can be omitted. Then, the asymptotic complexity of the MAP-MSDD of a 2^p-DPSK scheme becomes $\mathcal{O}[p\cdot 2^{(p(N-1))}]$. Therefore, employing the brute-force search carried out by the MAP-MSDD, might impose a potentially excessive computational complexity and hence may preclude its practical implementation, especially for high-order modulation schemes and/or for high observation window sizes. For example, under the assumption of an observation window size of $N=6$ and the 16-DAPSK scheme of Fig. 2, the number of evaluations of the PDF $p(\mathbf{y}|\mathbf{\Gamma},\mathbf{\Theta})$ of (4) required for each 4-bit-coded symbol is as high as $2^{26} = 6.7109\times10^7$.

B. The Design of Iterative Amplitude/Phase MSDD

Recently, the SD mechanism has been successfully adopted for the MAP-MSDD of a DPSK modulated system [8] based on the fact that the transmitted signal matrix $\mathbf{X}_{\mathrm{d}}$ is unitary. This technique achieved a significant complexity reduction. Unfortunately, this SD-aided complexity reduction scheme cannot be directly applied for the DAPSK modulated system considered, since $\mathbf{X}_{\mathrm{d}}$ is no longer unitary. As another approach of reducing the complexity, the idea of decoupling the joint amplitude and phase detection was conceived in [6] for MSDD invoked for DAPSK modulated transmission over Rayleigh channels. Regretfully, this sub-optimum scheme achieved a complexity reduction at the cost of a significant performance loss. Hence, we would like to tackle the challenging issue of implementing MAP-MSDD for the DAPSK scheme at a substantially reduced complexity.

To recover this potentially substantial performance degradation imposed by the sub-optimum scheme proposed in [6], here a novel iterative A/P MSDD (IAP-MSDD) mechanism is proposed for channel coded DAPSK modulated systems, where specifically tailored information may be iteratively exchanged between the decoupled serially concatenated multiple-symbol differential amplitude detector (MSDAD) and multiple-symbol differential phase detector (MSDPD), as illustrated in Fig. 3. Specifically, N consecutively received symbols are collected and fed through both the MSDAD and MSDPD of Fig. 3, where the soft-decision-based detection of the amplitude- and phase-modulation-related bits is conducted independently and iteratively. In the presence of the transmit-domain phase information $\hat{\mathbf{\Theta}}$, the *a posteriori* amplitude-modulation-related bit LLRs may be computed by the MSDAD as:

$$L_D(b_{\gamma,i}^n|\mathbf{y},\hat{\mathbf{\Theta}}) = \ln\frac{\Pr(b_{\gamma,i}^n=+1|\mathbf{y},\hat{\mathbf{\Theta}})}{\Pr(b_{\gamma,i}^n=-1|\mathbf{y},\hat{\mathbf{\Theta}})} = \ln\frac{\sum_{\mathbf{b}_\gamma\in\mathbb{B}_{n,i,+1}^\gamma} p(\mathbf{y}|\mathbf{\Gamma},\hat{\mathbf{\Theta}})\Pr(\mathbf{\Gamma}|\hat{\mathbf{\Theta}})}{\sum_{\mathbf{b}_\gamma\in\mathbb{B}_{n,i,-1}^\gamma} p(\mathbf{y}|\mathbf{\Gamma},\hat{\mathbf{\Theta}})\Pr(\mathbf{\Gamma}|\hat{\mathbf{\Theta}})}, \tag{7}$$

$$= \ln\frac{\sum_{\mathbf{b}_\gamma\in\mathbb{B}_{n,i,+1}^\gamma} p(\mathbf{y}|\mathbf{\Gamma},\hat{\mathbf{\Theta}})\Pr(\mathbf{b}_\gamma)}{\sum_{\mathbf{b}_\gamma\in\mathbb{B}_{n,i,-1}^\gamma} p(\mathbf{y}|\mathbf{\Gamma},\hat{\mathbf{\Theta}})\Pr(\mathbf{b}_\gamma)}, \tag{8}$$

where $\mathbb{B}_{n,i,\pm1}^\gamma$ represents the set of $2^{[q(N-1)-1]}$ legitimate amplitude-modulation-related MSB vectors $\mathbf{b}_\gamma$ associated with $b_{\gamma,i}^n=\pm1$ ($i\in\{1,\cdots,q\}$). Initially, when the phase information $\hat{\mathbf{\Theta}}$ is not available from the MSDPD, the initial phase information is obtained based on the output of the phase detector as $\hat{\mathbf{\Theta}}=[\phi_0,\cdots,\phi_{(N-1)}]^T$ by toggling the phase information feedback switch to the '1' location of Fig. 3, in order to neglect the phase error in the first round of MSDAD detection. Then, the amplitude ratios stored in $\hat{\mathbf{\Gamma}}$ may be calculated relying on the DASK processing of the *a posteriori* amplitude-modulation-related bit LLRs, i.e. $L_D(\mathbf{b}_\gamma|\mathbf{y},\hat{\mathbf{\Theta}})$ of (7), which are

next delivered to the serially concantenated MSDPD. Similarly, with the aid of the amplitude ratio estimates $\hat{\mathbf{\Gamma}}$, the *a posteriori* phase-modulation-related bit LLRs $L_D(\mathbf{b}_\theta|\mathbf{y},\hat{\mathbf{\Gamma}})$ may be computed by the MSDPD as follows:

$$L_D(b^n_{\theta,i}|\mathbf{y},\hat{\mathbf{\Gamma}}) = \ln \frac{\sum_{\mathbf{b}_\theta \in \mathbb{B}^\theta_{n,i,+1}} p(\mathbf{y}|\hat{\mathbf{\Gamma}},\mathbf{\Theta})\Pr(\mathbf{b}_\theta)}{\sum_{\mathbf{b}_\theta \in \mathbb{B}^\theta_{n,i,-1}} p(\mathbf{y}|\hat{\mathbf{\Gamma}},\mathbf{\Theta})\Pr(\mathbf{b}_\theta)}, \tag{9}$$

where $\mathbb{B}^\theta_{n,i,\pm 1}$ denotes the set of $2^{[(p-q)(N-1)-1]}$ legitimate phase-modulation-related bit vectors $\mathbf{b}_\theta$ associated with $b^n_{\theta,i} = \pm 1$ ($i \in \{1,\cdots,p-q\}$). From the second iteration of the MSDAD process, the phase information feedback switch is toggled to the '2' position, since $\hat{\mathbf{\Theta}}$ in (7) can be computed based on the DPSK processing of the *a posteriori* phase-modulation-related bit LLRs, $L_D(\mathbf{b}_\theta|\mathbf{y},\hat{\mathbf{\Gamma}})$ of (9), delivered by the MSDPD of Fig. 3, in the interest of exploiting the improved-confidence phase information in the MSDAD detection.

In our investigations we found that the conditional autocorrelation matrix $\Psi(\mathbf{X}_\mathrm{d})$ is dependent on a_ref, but not on s_ref. Hence, a further complexity reduction may be achieved by averaging $p(\mathbf{y}|\mathbf{X}_\mathrm{d})$ over all possible a_ref values instead of x_ref, when computing the $p(\mathbf{y}|\mathbf{\Gamma},\mathbf{\Theta})$ of (4). Thus, the burden of computing $p(\mathbf{y}|\mathbf{\Gamma},\hat{\mathbf{\Theta}})$ in (8) and $p(\mathbf{y}|\hat{\mathbf{\Gamma}},\mathbf{\Theta})$ in (9) can be reduced by a factor of $2^{(p-q)}$ using

$$p(\mathbf{y}|\hat{\mathbf{\Gamma}},\mathbf{\Theta}) = \mathcal{E}_{a_\mathrm{ref}}\{p(\mathbf{y}|\mathbf{X}_\mathrm{d})\}, \tag{10}$$

instead of using (4). Consequently, the asymptotic complexity per iteration of the proposed IAP-MSDD scheme for the 2^p-DAPSK scheme using 2^q concentric-ring constellation is $\mathcal{O}(q\cdot 2^{(qN)} + (p-q)\cdot 2^{(p-q)(N-1)+q}))$. Hence, by assuming $N = 6$ and 16-DAPSK, the number of evaluations of (4) required for each symbol in the IAP-MSDD process becomes $2^6 + 3\times 2^{16} = 1.9667\times 10^5$ per iteration (99.97% of the total complexity is contributed by the phase-modulation-related bit detection). This total complexity is two orders of magnitude lower than that of the traditional full-search-based MSDD.

IV. Complexity Reduction Strategies for the IAP-MSDD

Although a substantial complexity reduction can be attained, the complexity imposed by the IAP-MSDD of Fig. 3 proposed for the DAPSK may still be deemed to be excessive, as illustrated in Section III-B, thus preventing its implementation in most pratical scenarios. Hence, we continue our quest for more efficient complexity reduction techniques designed for the IAP-MSDD, in particular for its computationally more demanding MSDPD stage, which contributes the majority of the total complexity imposed.

A. Estimation of the Transmit-Domain Symbol Amplitude

According to (10), an immediate further complexity reduction by a factor of 2^q may be achieved at the MSDPD stage, if the amplitudes $\hat{\mathbf{A}}_{\rm d}$ of the transmitted symbols, instead of the amplitude ratios $\hat{\mathbf{\Gamma}}$, are estimated on the basis of the *a posteriori* LLRs $L_D(\mathbf{b}_\gamma^n|\mathbf{y},\hat{\mathbf{\Theta}})$ provided by the MSDAD detector. This is because in the presence of the amplitude estimates $\hat{\mathbf{A}}_{\rm d}$, the MSDPD detector may become capable of approximately computing the *a posteriori* LLRs $L_D(\mathbf{b}_\theta^n|\mathbf{y},\hat{\mathbf{\Gamma}})$ without averaging over all possible amplitudes of the reference symbol by using

$$L_D(b_{\theta,i}^n|\mathbf{y},\hat{\mathbf{\Gamma}}) \approx L_D(b_{\theta,i}^n|\mathbf{y},\hat{\mathbf{A}}_{\rm d}) = \ln\frac{\Pr(b_{\theta,i}^n=+1|\mathbf{y},\hat{\mathbf{A}}_{\rm d})}{\Pr(b_{\theta,i}^n=-1|\mathbf{y},\hat{\mathbf{A}}_{\rm d})}, \tag{11}$$

$$= \ln\frac{\sum_{\mathbf{b}_\theta\in\mathbb{B}_{n,i,+1}^\theta} p(\mathbf{y}|\hat{\mathbf{A}}_{\rm d},\mathbf{\Theta})\Pr(\mathbf{b}_\theta)}{\sum_{\mathbf{b}_\theta\in\mathbb{B}_{n,i,-1}^\theta} p(\mathbf{y}|\hat{\mathbf{A}}_{\rm d},\mathbf{\Theta})\Pr(\mathbf{b}_\theta)}, \tag{12}$$

where we have

$$p(\mathbf{y}|\hat{\mathbf{A}}_{\rm d},\mathbf{\Theta}) = p[\mathbf{y}|\tilde{\mathbf{X}}_{\rm d}=\hat{\mathbf{A}}_{\rm d}\times\mathbf{S}_{\rm d}(\mathbf{\Theta})], \tag{13}$$

with the diagonal matrix $\mathbf{S}_{\rm d}(\mathbf{\Theta})$ containing the N-component DPSK symbols along its diagonal associated with the phase difference information $\mathbf{\Theta}$. Bearing in mind the benefit of acquiring the transmit-domain symbol amplitude estimates, we further elaborate on the amplitude estimation procedure, constituted by the following two major steps:

Step 1: Estimate the amplitude, $a_{\rm ref}$, of the reference symbol, namely, the first symbol x_0, of the block of N successively transmitted symbols on the basis of the amplitude ratio $\hat{\mathbf{\Gamma}}$ and phase difference estimates $\hat{\mathbf{\Theta}}$, provided by the MSDAD and MSDPD detectors, respectively.

Since we have $\Pr(a_{\rm ref}=\alpha^k|\hat{\mathbf{\Gamma}},\hat{\mathbf{\Theta}}) = \Pr(a_{\rm ref}=\alpha^k) = 2^{-q}, k\in\{0,\cdots,2^q-1\}$, the *soft-decision-based* amplitude of the reference symbol may be calculated by exploiting Bayes' theorem as:

$$\begin{aligned}
\hat{a}_{\rm ref} &= \sum_{k=0}^{2^q-1}\alpha^k\cdot\Pr(\breve{a}_{\rm ref}=\alpha^k|\mathbf{y},\hat{\mathbf{\Gamma}},\hat{\mathbf{\Theta}}),\\
&= \sum_{k=0}^{2^q-1}\frac{\alpha^k\cdot p(\mathbf{y}|\breve{a}_{\rm ref}=\alpha^k,\hat{\mathbf{\Gamma}},\hat{\mathbf{\Theta}})\Pr(\breve{a}_{\rm ref}=\alpha^k)}{\sum_{l=0}^{2^q-1}p(\mathbf{y}|\breve{a}_{\rm ref}=\alpha^l,\hat{\mathbf{\Gamma}},\hat{\mathbf{\Theta}})\Pr(\breve{a}_{\rm ref}=\alpha^l)},\\
&= \sum_{k=0}^{2^q-1}\frac{\alpha^k\cdot p(\mathbf{y}|\breve{a}_{\rm ref}=\alpha^k,\hat{\mathbf{\Gamma}},\hat{\mathbf{\Theta}})}{\sum_{l=0}^{2^q-1}p(\mathbf{y}|\breve{a}_{\rm ref}=\alpha^l,\hat{\mathbf{\Gamma}},\hat{\mathbf{\Theta}})},\\
&= \sum_{k=0}^{2^q-1}\frac{\alpha^k\cdot p(\mathbf{y}|\hat{\mathbf{A}}_{\rm d}^k,\hat{\mathbf{\Theta}})}{\sum_{l=0}^{2^q-1}p(\mathbf{y}|\hat{\mathbf{A}}_{\rm d}^l,\hat{\mathbf{\Theta}})},
\end{aligned} \tag{14}$$

where the diagonal matrix $\hat{\mathbf{A}}_{\rm d}^k$ contains the transmitted symbols' amplitude estimates along its diagonal associated

with its first diagonal element $a_0 = \check{a}_{\rm ref} = \alpha^k$. Then, the diagonal elements of $\hat{\mathbf{A}}_{\rm d}^k$ may be calculated recursively:

$$\hat{a}_{n+1} = \sum_{\check{\gamma}_{n+1}\in\mathcal{R},\check{a}_n\in\mathcal{A}} \alpha^{(i_{\rm A}\{\check{\gamma}_{n+1}\}+i_{\rm A}\{\check{a}_n\})\bmod 2^q} \cdot \Pr(\check{\gamma}_{n+1}) \cdot \Pr(\check{a}_n), \tag{15}$$

where the ASK symbol probability $\Pr(\check{\gamma}_{n+1})$ may be readily calculated based on the *a posteriori* ASK-modulation-related bit LLRs, i.e., on $L_D(\mathbf{b}_\gamma^{n+1}|\mathbf{y},\hat{\mathbf{\Theta}})$ of (7) generated by the MSDAD, while the DASK symbol probability $\Pr(\check{a}_n)$ can be approximately evaluated as:

$$\Pr(\check{a}_n = \alpha^k) \approx \begin{cases} 1, & \text{for } \hat{a}_n \leq \alpha^k,\ k=0; \\ \frac{\hat{a}_n - \alpha^{k-1}}{\alpha^{k+1}-\alpha^k}, & \text{for } \alpha^{k-1} \leq \hat{a}_n \leq \alpha^k; \\ \frac{\alpha^{k+1}-\hat{a}_n}{\alpha^{k+1}-\alpha^k}, & \text{for } \alpha^k < \hat{a}_n < \alpha^{k+1}; \\ 0, & \text{for all the other cases,} \end{cases} \tag{16}$$

which essentially reduces the computational complexity imposed by (15), especially when the size of $\mathcal{A}$ is high.

Step 2: Upon obtaining the amplitude estimate for the reference symbol from (14), we estimate the amplitudes of the remaining $(N-1)$ transmitted symbols of the specific multiple-symbol block with the aid of the amplitude ratio estimates $\hat{\mathbf{\Gamma}}$.

More specifically, in order to generate $\hat{\mathbf{A}}_{\rm d}$ for the MSDPD detection of (11), the soft-decision-based amplitude calculation criterion of (15) - which was employed when obtaining $\hat{\mathbf{A}}_{\rm d}^k$ of (14) - is also invoked for recursively computing the diagonal elements of the matrix $\hat{\mathbf{A}}_{\rm d}$ commencing from the first element $\hat{a}_{\rm ref}$ of (14).

B. Incorporating a Structured Tree Search in the MSDPD Stage

As another benefit of estimating the amplitudes of the transmitted symbols, an efficiently structured tree search employed by the well-known SD may be incorporated into the computationally demanding MSDPD stage, as detailed in this section. We will demonstrate that this technique is capable of achieving a further significant complexity reduction. Provided that the amplitude estimate matrix $\hat{\mathbf{A}}_{\rm d}$ has been obtained, we now further elaborate on (13) by reformulating it as follows (the argument $\mathbf{\Theta}$ in $\mathbf{S}_{\rm d}(\mathbf{\Theta})$ is omitted for notational simplicity):

$$p(\mathbf{y}|\tilde{\mathbf{X}}_d = \hat{\mathbf{A}}_{\rm d}\mathbf{S}_{\rm d}) = \frac{\exp\{-\mathbf{y}^{\rm H}[\Psi(\tilde{\mathbf{X}}_{\rm d})]^{-1}\mathbf{y}\}}{\pi^N \det[\Psi(\tilde{\mathbf{X}}_{\rm d})]}, \tag{17}$$

where according to (5) we have:

$$\Psi(\tilde{\mathbf{X}}_{\mathrm{d}}) = \Psi(\mathbf{S}_{\mathrm{d}}) = \hat{\mathbf{A}}_{\mathrm{d}}\mathbf{S}_{\mathrm{d}}\boldsymbol{\Sigma}_h(\hat{\mathbf{A}}_{\mathrm{d}}\mathbf{S}_{\mathrm{d}})^{\mathrm{H}} + 2\sigma_w^2\mathbf{I}_N, \tag{18}$$

$$= \mathbf{S}_{\mathrm{d}}(\tilde{\boldsymbol{\Sigma}}_h + 2\sigma_w^2\mathbf{I}_N)\mathbf{S}_{\mathrm{d}}^{\mathrm{H}}, \tag{19}$$

with $\tilde{\boldsymbol{\Sigma}}_h \triangleq \hat{\mathbf{A}}_{\mathrm{d}}\boldsymbol{\Sigma}_h\hat{\mathbf{A}}_{\mathrm{d}}^{\mathrm{H}}$ being termed as the *equivalent* channel covariance matrix. Note that for a given $\hat{\mathbf{A}}_{\mathrm{d}}$, the denominator of (17) is independent of $\mathbf{S}_{\mathrm{d}}$, since $\mathbf{S}_{\mathrm{d}}$ is unitary, i.e. we have $\mathbf{S}_{\mathrm{d}}^{-1} = \mathbf{S}_{\mathrm{d}}^{\mathrm{H}}$. Thus, using the Max-log approximation, the calculation of the *a posteriori* phase-modulation-related bit LLRs of (12) may be simplified as:

$$L_D(\hat{b}_{\theta,i}^n) \approx \max_{\mathbf{b}_\theta \in \mathbb{B}_{n,i,+1}^{\theta}} \left\{-\mathbf{y}^{\mathrm{H}}[\Psi(\tilde{\mathbf{X}}_{\mathrm{d}})]^{-1}\mathbf{y} + \ln \Pr(\boldsymbol{\Theta})\right\} - \max_{\mathbf{b}_\theta \in \mathbb{B}_{n,i,-1}^{\theta}} \left\{-\mathbf{y}^{\mathrm{H}}[\Psi(\tilde{\mathbf{X}}_{\mathrm{d}})]^{-1}\mathbf{y} + \ln \Pr(\boldsymbol{\Theta})\right\}. \tag{20}$$

Furthermore, since $\mathbf{S}_{\mathrm{d}}$ is unitary and owing to the independence of the elements of $\boldsymbol{\Theta}$, we finally arrive at:

$$L_D(\hat{b}_{\theta,i}^n) \approx \max_{\mathbf{b}_\theta \in \mathbb{B}_{n,i,+1}^{\theta}} \left\{-||\mathbf{L}^{\mathrm{T}}\mathbf{Y}_{\mathrm{d}}^{\mathrm{H}}\mathbf{s}||^2 + \sum_{n=0}^{N-2} \ln \Pr(\theta_n)\right\} - \max_{\mathbf{b}_\theta \in \mathbb{B}_{n,i,-1}^{\theta}} \left\{-||\mathbf{L}^{\mathrm{T}}\mathbf{Y}_{\mathrm{d}}^{\mathrm{H}}\mathbf{s}||^2 + \sum_{n=0}^{N-2} \ln \Pr(\theta_n)\right\}, \tag{21}$$

where we have $\mathbf{Y}_{\mathrm{d}} \triangleq \mathrm{diag}\{\mathbf{y}\}$ and the lower triangular matrix $\mathbf{L}$ satisfying $\mathbf{L}\mathbf{L}^{\mathrm{H}} = (\tilde{\boldsymbol{\Sigma}}_h + 2\sigma_w^2\mathbf{I}_N)^{-1}$ may be obtained by the Cholesky factorization of the symmetric positive definite matrix $(\tilde{\boldsymbol{\Sigma}}_h + 2\sigma_w^2\mathbf{I}_N)^{-1}$ of (19). By defining the upper triangular matrix $\mathbf{U} = \mathbf{L}^{\mathrm{T}}\mathbf{Y}_{\mathrm{d}}^{\mathrm{H}}$ and after a few straightforward manipulations, we finally have:

$$L_D(\hat{b}_{\theta,i}^n) \approx \max_{\mathbf{b}_\theta \in \mathbb{B}_{n,i,+1}^{\theta}} \left\{\sum_{n=0}^{N-2}\left(\ln \Pr(\theta_n) - \sum_{m=n}^{N-1}|u_{nm}s_m|^2\right)\right\} - \max_{\mathbf{b}_\theta \in \mathbb{B}_{n,i,-1}^{\theta}} \left\{\sum_{n=0}^{N-2}\left(\ln \Pr(\theta_n) - \sum_{m=n}^{N-1}|u_{nm}s_m|^2\right)\right\}, \tag{22}$$

where u_{nm} is the element of matrix $\mathbf{U}$ located in the nth row and mth column. Consequently, thanks to the upper-triangular structure of the matrix $\mathbf{U}$, we may find the two maximum values in (22) with the aid of the efficient tree-search-based SD algorithm of [8].

V. Performance Evaluation and Discussions

In order to visualize the EXtrinsic Information Transfer (EXIT) charateristics [13] of the proposed IAP-MSDSD scheme, in Fig. 4 we plot the EXIT curves associated with different observation window sizes of N for the IAP-MSDSD against those of the CDD and of the traditional MSDD. Under the assumption of the 16-DAPSK modulated system of Fig. 1 and a normalized Doppler frequency of $f_d = 0.01$, the EXIT curves of Fig. 4 are obtained by evaluating the *extrinsic* mutual information (MI), I_E, at the output of the specific differential detector for a given

input stream of bit LLRs along with the *a priori* MI I_A. According to the area properties of the EXIT chart [13], the upwards-shifted EXIT curve of the IAP-MSDSD in Fig. 4 suggests that a significantly higher maximum transmission rate may be achieved in comparison to the CDD assisted system using $N = 2$. This throughput gain was achieved by jointly detecting $N > 2$ data symbols using the IAP-MSDSD, as also visualized in the 3D plot of Fig. 5, where the maximum achievable throughput of the IAP-MSDSD-aided 16-DAPSK modulated system is portrayed versus both the SNR and the ring-ratio α. Additionally, thanks to the IAP-based detection regime, the multiple-symbol detection mechanism may be employed in only one of its two detection phases, namely in either the amplitude or the phase detection phases for the sake of striking a compromise between the achievable performance and the complexity imposed. This yields the combined MSDAD and conventional differential phase detection (CDPD) as well as the amalgamated conventional differential amplitude detection (CDAD) and MSDPD mechanisms. Consequently, a reduced complexity may be imposed by these two hybrid detectors in comparison to the IAP-MSDSD at the cost of a compromised iteration gain, as indicated by the associated downwards-shifted dotted and dot-dashed EXIT curves in Fig. 4. Moreover, as implied by the almost invisible gap between the EXIT curve of the IAP-MSDSD and that of the traditional MSDD seen in Fig. 4, both the MSDAD and MSDPD of the IAP-MSDSD of Fig. 3 has to be activated only once, in order to approach the performance of the traditional MSDD. In other words, the MSDAD operation based on the output of the phase detector formulated as $\hat{\mathbf{\Theta}} = [\phi_0, \cdots, \phi_{(N-1)}]^T$, which is generated by toggling the phase information feedback switch to the '1' position of Fig. 3, is capable of delivering sufficiently useful transmit-domain symbol amplitude estimates for the subsequent MSDPD. Hence, this observation allows us to set the number of iterations between the MSDAD and MSDPD stages to one in our simulations throughout the paper in order to avoid any unnecessary operations. Thus, remarkablely, the complexity imposed by the IAP-MSDSD becomes about five orders of magnitude lower than that of the traditional MSDSD in the context of the 16-DAPSK modulation-aided system across a wide range of SNRs, as seen in Fig. 6, where the complexity quantified in terms of the number of transmitted symbol vector candidate enumerations during the differential detection is portrayed versus both the SNR and the ring-ratio α. Furthermore, observe from the IAP-MSDSD-related throughput and complexity surfaces plotted in Figs. 5 and 6, respectively, that the ring-ratio α employed by 16-DAPSK plays a crucial role in determining both the system's achievable transmission rate as well as its detection complexity. Specifically, the simulation results seen in Figs. 5 and 6 suggest that setting the ring-ratio to $\alpha \approx 2.0$ constitutes

an appropriate choice for maximizing the achievable throughput [14], while minimizing the complexity imposed.

VI. Conclusions

In this paper, we proposed an IAP-MSDSD scheme for DAPSK modulated systems, which was shown to be capable of achieving a near-MAP-MSDD performance at a substantially reduced complexity, that was about five orders of magnitude lower than that imposed by the traditional MAP-MSDD in the case of 16-DAPSK.

References

[1] K. Etemad, "Overview of mobile WiMAX technology and evolution," *IEEE Communications Magazine*, vol. 46, pp. 31–40, Oct. 2008.

[2] K. Etemad, "Multisite filed trial for LTE and advanced concepts," *IEEE Communications Magazine*, vol. 47, no. 2, pp. 92–98, 2009.

[3] W. T. Webb, L. Hanzo, and R. Steele, "Bandwidth efficient QAM schemes for Rayleigh fading channels," *IEE Proceedings I, Communications, Speech and Vision*, vol. 138, pp. 169–175, June 1991.

[4] H. Rohling and V. Engels, "Differential amplitude phase shift keying (DAPSK) - a new modulation method for DTVB," *Proceedings of International Broadcasting Convention*, pp. 102–108, 1995.

[5] M. Machida, S. Handa, and S. Oshita, "Multiple-symbol differential detection of APSK based on MAP criterion," *IEEE Global Telecommunications Conference*, vol. 5, pp. 2740–2744, Nov. 1998.

[6] K. Ishibashi, H. Ochiai, and R. Kohno, "Low-complexity bit-interleaved coded DAPSK for Rayleigh-fading channels," *IEEE Journal on Selected Areas in Communications*, vol. 23, pp. 1728–1738, Sept. 2005.

[7] R. F. H. Fischer, L. H. J. Lampe, and S. H. M. Weinfurtner, "Coded modulation for noncoherent reception with application to OFDM," *IEEE Transactions on Vechicular Technology*, vol. 50, pp. 910–919, July 2001.

[8] V. Pauli, L. Lampe, and R. Schober, ""Turbo DPSK" using soft multiple-symbol differential sphere decoding," *IEEE Transactions on Information Theory*, vol. 52, no. 4, pp. 1385–1398, 2006.

[9] L. Hanzo, Y. Akhtman, L. Wang, and M. Jiang, *MIMO-OFDM for LTE, WIFI and WIMAX: Coherent versus Non-Coherent and Cooperative Turbo-Transceivers*. John Wiley and IEEE Press, 2010.

[10] D. D. Liang, S. X. Ng, and L. Hanzo, "Soft-decision star-QAM aided BICM-ID," *IEEE Signal Processing Letters*, vol. 18, pp. 169–172, Jan. 2011.

[11] Y. C. Chow, A. R. Nix, and J. P. McGeehan, "Analysis of 16-APSK modulation in AWGN and Rayleigh fading channel," *Electronics Letters*, vol. 28, no. 17, pp. 1608–1610, 1992.

[12] L. Xiao, X. Dong, and T. T. Tjhung, "On the maximum likelihood detection of DAPSK signaling," *IEEE Vehicular Technology Conference (VTC'04-Fall)*, vol. 2, pp. 1258–1262, 2004.

[13] A. Ashikhmin, G. Kramer, and S. ten Brink, "Extrinsic information transfer functions: model and erasure channel properties," *IEEE Transactions on Information Theory*, vol. 50, pp. 2657–2673, Nov. 2004.

[14] L. Lampe and R. Fischer, "Comparison and optimization of differentially encoded transmission on fading channels," *in Proc. 3rd Int. Symp. Power-Line Communications (ISPLC)*, 1999.

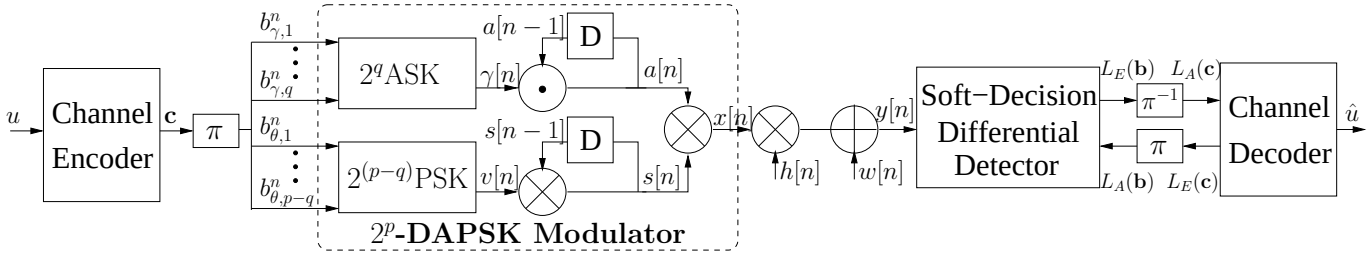

Fig. 1. Overall system model of bit-interleaved coded 16-DAPSK over Rayleigh-fading channel.

TABLE I
AMPLITUDE MAPPING FOR 16- AND 64-DAPSK

16-DAPSK ($q=1$)				**64-DAPSK ($q=2$)**					
$a[n]$		$b^n_{\gamma,1}$		$a[n]$		$b^n_{\gamma,1}, b^n_{\gamma,2}$			
		0	1			00	01	11	10
		$\gamma[n]$				$\gamma[n]$			
		1	α			1	α	α^2	α^3
$a[n-1]$	1	1	α	$a[n-1]$	1	1	α	α^2	α^3
					α	α	α^2	α^3	1
	α	α	1		α^2	α^2	α^3	1	α
					α^3	α^3	1	α	α^2

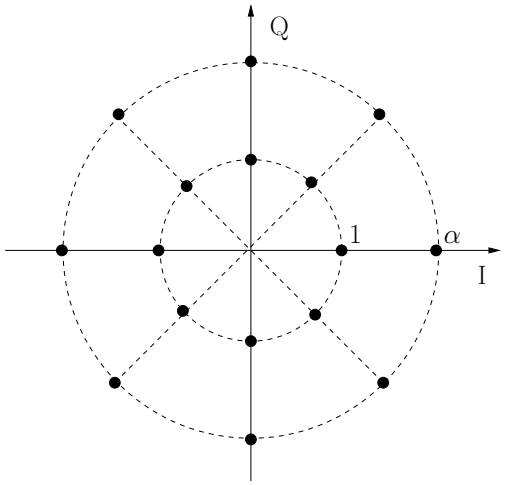

Fig. 2. Signal constellation of 16-DAPSK (α denotes the ring ratio).

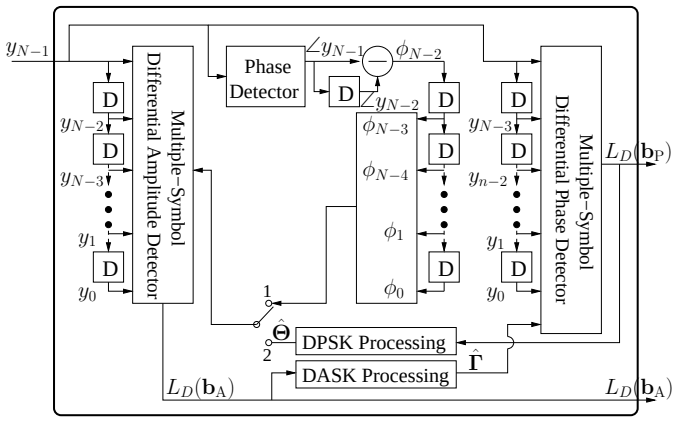

Fig. 3. Iterative Multiple-Symbol Differential Amplitude/Phase Detection (Illustration for the first multiple-symbol block, i.e., $k_N = 0$).

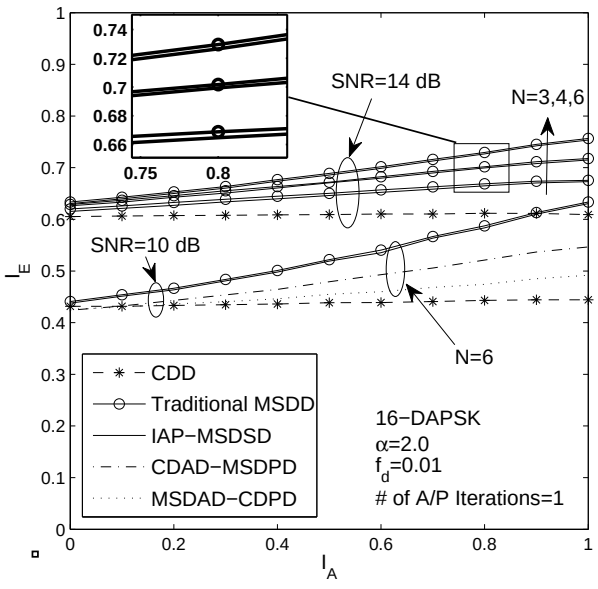

Fig. 4. EXIT chart of the IAP-MSDSD employed in the 16-DAPSK system.

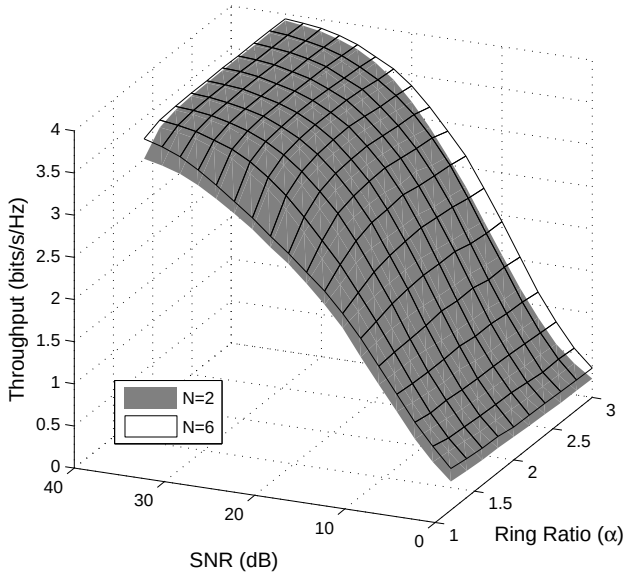

Fig. 5. Maximum achievable throughput of the 16-DAPSK system.

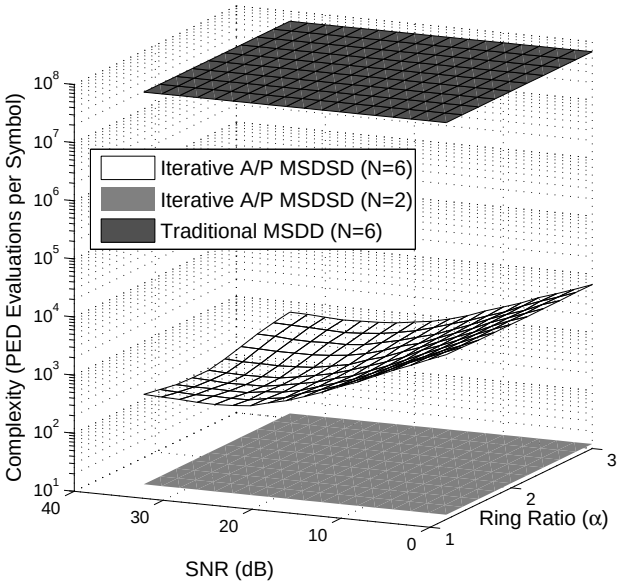

Fig. 6. Complexity reduction achieved by the IAP-MSDSD in the 16-DAPSK system.